



Universiteit
Leiden
The Netherlands

Novel applications of objective measures in cochlear implants

Dong, Y.

Citation

Dong, Y. (2022, February 15). *Novel applications of objective measures in cochlear implants*. Retrieved from <https://hdl.handle.net/1887/3275097>

Version: Publisher's Version

License: [Licence agreement concerning inclusion of doctoral thesis in the Institutional Repository of the University of Leiden](#)

Downloaded from: <https://hdl.handle.net/1887/3275097>

Note: To cite this publication please use the final published version (if applicable).

Chapter 5

**Short and long-latency components of the eCAP
reveal different refractory properties**

Yu Dong, Jeroen J. Briaire, H. Christiaan

Stronks and Johan H. M. Frijns

Submitted to Hearing Research

Abstract

Background: The refractory recovery function (RRF) measures the electrically evoked compound action potential (eCAP) in response to a second pulse (probe) after masking by a first pulse (masker). This RRF is usually used to assess the refractory properties of the electrically stimulated auditory nerve (AN) by recording the eCAP amplitude as a function of the masker probe interval. Instead of assessing eCAP amplitudes only, recorded waveforms can also be described as a combination of a short-latency component (S-eCAP) and a long-latency component (L-eCAP). It has been suggested that these two components originate from two different AN fiber populations with differing refractory properties. The main objective of this study was to explore whether the refractory characteristics revealed by S-eCAP, L-eCAP, and the raw eCAP (R-eCAP) differ from each other. For clinical relevance, we compared these refractory properties between children and adults and examined whether they are related to cochlear implant (CI) outcomes.

Design: In this retrospective study, the raw RRF (R-RRF) was obtained from 121 Hi-Focus Mid-Scala or IJ cochlear implant (Advanced Bionics, Valencia, CA) recipients. Each R-eCAP of the R-RRF was split into an S-eCAP and an L-eCAP using deconvolution to produce two new RRFs: S-RRF and L-RRF. The refractory properties were characterized by fitting an exponential decay function with three parameters: the absolute refractory period (T); the saturation level (A); and the speed of recovery from nerve refractoriness (τ), i.e., a measure of the relative refractory period. We compared the parameters of the R-RRF (T_R , A_R , and τ_R) with those obtained from the S-RRF (T_S , A_S , and τ_S) and L-RRF (T_L , A_L , and τ_L) and investigated whether these parameters differed between children and adults. In addition, we examined the associations between these parameters and speech perception in adults with CI. Linear mixed modeling was used for the analyses.

Results: We found that T_R was significantly longer than T_S and T_L , and T_S was significantly longer than T_L . A_R was significantly larger than A_S and A_L , and A_S was significantly larger

than A_L . Also, τ_S was significantly longer in comparison to τ_R and τ_L , but no significant difference was found between τ_R and τ_L . Children presented a significantly larger A_S and A_L and a shorter T_R and T_S in comparison to adults. Shorter τ_S was significantly associated with better speech perception in adult CI recipients, but other parameters were not.

Conclusion: We demonstrated that the two components of the eCAP have different refractory properties and that these also differ from those of the R-eCAP. In comparison with the R-eCAP, the refractory properties derived from the S-eCAP and L-eCAP can reveal additional clinical implications in terms of the refractory difference between children and adults as well as speech performance after implantation. Thus, it is worthwhile considering the two components of the eCAP in the future when assessing the clinical value of the auditory refractory properties.

Keywords: Cochlear implants, auditory nerve, sensorineural hearing loss, refractory recovery, electrically evoked action potential, speech perception

5.1 Introduction

A cochlear implant (CI) is an intracochlear device that can partially restore the hearing functionality of patients with severe-to-profound hearing loss. A CI transforms a sound signal into electrical stimuli that directly activate the auditory nerve (AN) inside the cochlea (Hughes, 2012). Previous studies reported that the neural refractoriness of the AN can affect its capability of accurately encoding temporal information (e.g., Gray, 1967; Wilson et al., 1994; Brown et al., 1990; Boulet et al., 2015; He et al., 2017) and is relevant to the functionality of the AN as well as speech perception (e.g., Stypulkowski and van den Honert, 1984; Wilson et al., 1994; He et al., 2017).

A common approach to exploring the refractory characteristics of the AN is to measure the refractory recovery function (RRF) of the electrically evoked compound action potential (eCAP) using a masker-probe artifact cancellation paradigm. In this paradigm, two pulses are applied, and the eCAP in response to the second pulse (the probe) is measured as a function of the masker

probe interval (MPI). The RRF can be obtained by plotting the eCAP amplitudes as a function of MPI (Miller et al., 2000; Morsnowski et al., 2006; Hey et al., 2017). Refractoriness arising from the first pulse (the masker) results in a masking of the eCAP triggered by the probe. In this paradigm, the eCAP is characterized by the amplitude of the main peaks, namely the difference between the first negative peak (N1) and the first positive peak (P1). The refractory properties of the AN can be obtained by fitting the RRF with an exponential function using three parameters: (1) the absolute refractory period (T); (2) the eCAP amplitude at the maximum saturation level (A); and (3) the relative refractory period (τ), which refers to the speed of recovery from relative refractoriness (e.g., Morsnowski et al., 2006; Botros and Psarros, 2010; He et al., 2017).

However, the method used in previous studies to assess the AN refractoriness is controversial (e.g., Miller et al., 2000; Morsnowski et al., 2006), because in this paradigm, the eCAP is characterized only by the amplitude of the main peaks. In considering the morphology of eCAPs, previous studies have observed two different types of eCAP waveforms (e.g., Van den Honert and Stypulkowski, 1984; Lai and Diller, 2000; Ramekers et al., 2015; van de Heyning et al., 2016; Dong et al., 2020). These waveforms can consist of either one negative and one positive peak or of two positive peaks that are similar in shape but differ in latencies (P1 and P2) (e.g., Lai and Dillier, 2000; He et al., 2017). The raw eCAP waveform (R-eCAP) can be described as a combination of a short-latency component (S-eCAP) and a long-latency component (L-eCAP). They may be attributed to a separate neural response of part of the AN fiber (ANF) population (Ramekers et al., 2015; Strahl et al., 2016; Konerding et al., 2020; Dong et al., 2020). This two-component concept was also supported by a single-fiber recording study in cats (Van den Honert and Stypulkowski, 1984). More importantly, the two groups of neural responses can be related to the survival and functional conditions of the AN. For instance, Strahl et al. (2016) suggested that the ratio between S-eCAP and L-eCAP can potentially indicate the survival condition of the AN. Stypulkowski and van den Honert (1984) reported that the refractory characteristics from the L-eCAP may be indicative of degeneration of the peripheral processes of the AN fibers based on their results recorded in cats. However, previous studies have not investigated whether the S-

eCAP and L-eCAP reveal different auditory refractory properties. We assumed that these two components arise from two different populations of ANFs, and therefore they may exhibit different refractory characteristics. Thus, in this study, we investigated the auditory refractory properties of the AN underlying the S-eCAP and L-eCAP.

Variation in terms of refractory characteristics of the AN between individuals and between different etiologies of deafness has been previously reported (e.g., Gantz et al., 1994; Fulmer et al., 2011; Van Eijl et al., 2017; He et al., 2017). Due to factors such as the duration of deafness and the maturation of the AN, differences in auditory refractory characteristics may be expected between young and adult CI users. For instance, in an animal study, the absolute refractory period of individual rat auditory neurons increased with the duration of deafness (Shepherd et al., 2001, 2004). Thus, a shorter absolute refractory period in children was anticipated, as children usually underwent a shorter duration of deafness in comparison to adults. To our knowledge, this has only been investigated by Carvalho et al. (2015), who reported no difference in refractory characteristics between children and adults except for the maximum saturation level. More importantly, earlier studies have not explored whether the auditory refractory characteristics underlying S-eCAP and L-eCAP in adults differ from or are the same as those in children.

Previous studies have attempted to explore whether the AN's speed of recovery from refractoriness is associated with the speech outcomes of adult CI recipients. These studies have not reported the effects of the absolute refractory period and saturation level on speech recognition, and results on the speed of recovery have been inconsistent. Some studies have reported that faster recovery from refractoriness derived from R-eCAP associates with better speech performance scores (Brown et al., 1990; Kiefer et al., 2001; Battmer et al., 2005; Fulmer et al., 2010), while other studies did not find such a relation (Abbas et al., 1991; Turner et al., 2002; Batter et al., 2005; Lee et al., 2012). One likely reason behind the incongruity is that previous studies only focused on the R-eCAP without considering the S-eCAP and L-eCAP separately.

Based on the above considerations, the first goal of the present study was to explore whether different refractory properties could be identified for the two components of the R-eCAP waveforms. To this end, the eCAP waveforms of the raw RRFs (R-RRFs) in a large group of CI patients were split into an S-eCAP and L-eCAP using iterative deconvolution (Dong et al., 2021). Using this method, two derived RRFs (S-RRF and L-RRF) were obtained from the R-RRFs, and the T, A, and τ parameters of the R-RRF, S-RRF and L-RRF were compared. Then, we investigated the potential clinical relevance of these refractory parameters, including (1) whether the parameters of the S-RRF, L-RRF, and R-RRF in children differed from those obtained from adult CI recipients and (2) whether these parameters can be indicative of speech outcomes in adult CI recipients.

5.2 MATERIAL AND METHODS

5.2.1 Patients

This retrospective study included 121 patients from the Leiden University Medical Centre (Leiden, the Netherlands) who received a CI between January 2010 and December 2015, and from whom intraoperative RRF recordings were available. These patients received a HiRes90K device (Advanced Bionics, Valencia, CA), either with a Mid-Scala or a 1J electrode array. Sixteen patients were excluded because of poor signal quality of eCAPs and failure of RRF fitting (see Data Recordings and Analysis) and the remaining 105 patients were included for further analyses. Table 5.1 shows the characteristics of the included patients.

5.2.2 Data recordings

The RRF recordings were conducted using a masker-probe artifact cancellation paradigm (Miller et al., 2000), which was provided by the Research Studies Platform Objective Measures software (Advanced Bionics, Valencia, CA). A schematic of this paradigm is shown in Figure 5.1. In this method, the masker-probe interval (MPI) systematically varies from 300 to 8000 μ s. The evoked

eCAP response to the partially masked probe (trace A) is recorded by a contact that is two electrodes apical to the stimulus. As the MPI increases, the AN gradually recovers from the refractory status induced by the masker, which leads to larger eCAPs at longer MPIs in trace A. The neural response and artifact evoked by the masker are measured (trace B). The artifact and the eCAP evoked by the probe pulse are derived by subtracting trace B from trace A (i.e., A-B). The reference MPI is set to minimize the neural response evoked by the probe pulse (trace C) (Morsnowski et al., 2006). Subtracting trace D from trace C (i.e., C-D) yields the artifact induced by the probe. The difference between the two derived traces (i.e., (A-B)-(C-D)) is the eCAP evoked by the first probe. The RRF was obtained by plotting the eCAP amplitudes as a function of MPIs. In the present study, the RRF recording was obtained using 13 MPIs (300, 398, 538, 721, 969, 1293, 1734, 2327, 3114, 4181, 5603, 750, 7995 μ s).

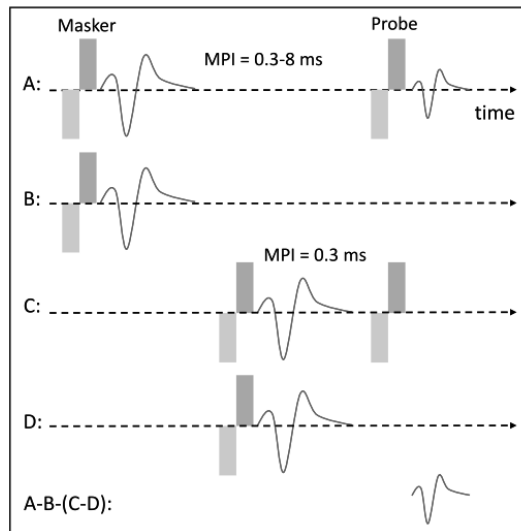


Fig. 5.1. A schematic illustration of the masker-probe artifact cancellation paradigm for measuring the eCAP refractory recovery function. Red solid lines indicate eCAP response. Colored rectangles indicate biphasic current pulses. Adapted from Miller et al. (2000). eCAPs: electrically evoked compound action potentials. MPI: masker probe interval.

The electrode arrays used in this study consisted of 16 contacts that were numbered from 1 to 16 in apical-to-basal order. RRF measurements were obtained at an apical electrode (E3), a middle

position (E8), and a basal position (E14). Due to time constraints in the operating theater, not all contacts could be recorded in all patients. Three stimulation electrode sites were recorded for 64 patients, two stimulation electrode sites (E3, E8) were recorded for 29 patients, and one stimulation site (E3) was recorded for 28 patients. The eCAPs were evoked using monopolar, charge-balanced, cathodic-first biphasic pulses (32 $\mu\text{s}/\text{phase}$) and recorded with a sampling rate of 56 kHz and a gain of 300. Raw eCAP recordings were low-pass filtered with a cutoff frequency of 8 kHz. N1 was defined as the minimum within the period from 180 to 490 μs , and P1 was the maximum from 470 to 980 μs after the end of stimulation. The eCAP amplitude was defined as the voltage difference between P1 and N1. The noise level was set to the average of the tail section of the recorded eCAP, i.e., the last 30 samples of the response. The signal-to-noise ratio was defined as the eCAP amplitude divided by the noise (Biesheuvel et al., 2017). eCAPs were in-or excluded using a semiautomatic method programmed using MATLAB (Mathworks 2019a, Natick, MA, USA), including two criteria: the eCAP amplitude had to be larger than 30 μV and the SNR had to exceed +15 dB. If the eCAPs did not meet both of these criteria, they were excluded. To ensure reliability, a stimulation site was excluded if more than 3 out of 13 eCAP waveforms of each R-RRF sequence did not meet these two criteria. As a result, 35 stimulation sites were excluded and the remaining 243 R-RRFs were used for extracting the S-RRF and L-RRF (see below).

5.2.3 Analysis

5.2.3.1 Extracting the S-eCAP and L-eCAP from the recorded eCAP

Under the assumption that each ANF generates the same unitary response, the R-eCAP can be described as a convolution of the unitary response with a compound discharge latency distribution consisting of two Gaussian components (for details, see Dong et al., 2021). The two Gaussian components represent the discharge latency distribution of the S-eCAP and the L-eCAP, respectively. To extract the S-eCAP and L-eCAP from the R-eCAP, two steps were performed. First, combined with a human unitary response, the compound discharge latency distribution was

derived from the R-eCAP using an iterative deconvolution model (Dong et al., 2020, 2021). Second, the S-eCAP and L-eCAP were simulated by convolving the first and second components of the compound discharge latency distribution with the human unitary response, respectively. The summation between the S-eCAP and L-eCAP mathematically equals the R-eCAP. We examined if this summation can accurately simulate the R-eCAP waveform by calculating the normalized root mean square error using MATLAB (Mathworks 2019a, Natick, MA, USA). Then, we determined the amplitudes of the S-eCAP and L-eCAP in the same manner as the R-eCAP amplitude. The S-RRF and L-RRF were obtained by plotting the amplitudes of S-eCAP and L-eCAP as a function of MPIs.

5.2.3.2 Deriving the refractory properties from R-RRF, S-RRF, and L-RRF

An exponential decay function was used to characterize the R-RRF, S-RRF, and L-RRF (e.g., Matsuoka et al., 2001; Morsnowski et al., 2006; Fulmer et al., 2010; Boulet et al., 2015).

$$RRF(MPI) = A * (1 - e^{(-\frac{MPI-T}{\tau})}) \quad (1)$$

T is the absolute refractory period (in μs), i.e., the minimum MPI for which an eCAP can be triggered by the probe. The amplitude recovers to the saturation level A (in μV) with a speed-of-recovery time constant τ (in μs). That is, τ represents the relative refractory period, reflecting the speed of recovery from relative refractoriness. T_R , A_R , and τ_R denote the parameters of R-RRF; T_S , A_S , and τ_S are those of S-RRF; and T_L , A_L , and τ_L are those of L-RRF. These parameters were calculated by fitting the R-RRF, S-RRF, and L-RRF using a least-squares curve fit with the Levenberg-Marquart algorithm using MATLAB (Mathworks 2019a, Natick, MA, USA). As the absolute refractory period cannot be shorter than $0 \mu\text{s}$, a stimulation site was excluded if any one of the parameters (T_R , T_S , or T_L) was smaller than $0 \mu\text{s}$, indicating a fitting error. As a result, 28 stimulation sites were excluded, and the remaining 215 sites originating from 105 patients were included for further statistical analyses.

5.2.4 Speech perception

Speech perception, defined as the word and phoneme recognition score obtained one year after implantation, was routinely evaluated for the adult CI recipients. The HiRes processing strategy from Advanced Bionics was applied to all patients. The speech material was presented at 65 dB SPL in a quiet listening environment. All speech testing was conducted in a soundproof room, using a calibrated sound speaker in a frontal position at a meter distance. The standard Dutch speech test of the Dutch Society of Audiology, consisting of phonetically balanced monosyllabic (CVC) word lists, was applied (Bosman & Smoorenburg, 1995). To enhance test reliability, four lists of 11 CVC words were administered. The number of words and phonemes that were correct was determined.

5.2.5 Statistics

In the present study, we used linear mixed modeling (LMM) for statistical analysis, because (1) LMMs have the advantage that they can account for random effects (e.g., between-subject variability), and (2) LMMs can also account for missing data that do not have to be random (Molenberghs et al., 1997; Fitzmaurice et al., 2004). We first tested whether the short and long-latency components of the eCAP reveal different refractory characteristics and whether they differ from those revealed by the raw eCAP waveform. To this end, three LMMs were constructed with each of the refractory parameters (i.e., T, A, and τ) as the dependent variable. To test whether the parameters derived from S-RRF and L-RRF differ from each other and from the ones obtained from R-RRF, a categorical fixed factor was introduced that reflected whether T, A, and τ were obtained from R-RRF, S-RRF, or L-RRF. An example model for parameter A is given as follows:

$$A = RSL + contact + 1|subject ID \quad (5.2)$$

where A is the dependent variable; RSL is the categorical variable with three levels (R, S, and L)

corresponding to R-RRF, S-RRF, and L-RRF; the contact with the levels (E3, E8, and E14) is entered as a fixed-effect variable; and subject ID is entered as a random categorical variable, including a random intercept (Brauer and Curtin, 2018). The significance level of each comparison was adjusted to 0.017 using post hoc Bonferroni-corrected multiple comparisons t-testing (0.05 divided by 3 comparisons).

Then, we evaluated the clinical relevance of the refractory parameters derived from R-RRF, S-RRF, and L-RRF. To compare the refractory characteristics between children and adults, nine LMMs were constructed that incorporated the following dependent variables: T_R , A_R , τ_R , T_S , A_S , τ_S , T_L , A_L , and τ_L . In these analyses, the 106 patients were classified into a child group (≤ 16 years, $n=42$) and an adult group (>16 years, $n=64$) by age (see Table 5.1). This categorical variable was entered as a fixed effect factor with two levels (i.e., pediatric and adult). The electrode contact number and subject ID were entered in the same way as Eq. (5.2).

In addition, we investigated whether the refractory parameters obtained from R-RRF, S-RRF, and L-RRF are related to the speech perception of adult CI recipients. Again, nine LMMs were constructed in which the adults' speech performance was compared with the refractory parameters T_R , T_S , T_L , A_R , A_S , A_L , τ_R , τ_S , and τ_L , respectively. In our data set, only a single speech score was available, but we had multiple measures for the refractory metrics. We used reverse LMM constructions; that is, T_R , T_S , T_L , A_R , A_S , A_L , τ_R , τ_S , and τ_L were entered as the dependent variable and the monosyllabic word score was entered as a fixed covariate in each model. The electrode contact and subject ID were included as a fixed-effect variable and a random variable, respectively (see Eq. (5.2)). Additionally, the relationship between phoneme score and the refractory parameters was evaluated in the same way. LMM analyses were carried out using the lme4 package in R (R version 3.6.1, The R Foundation for Statistical Computing, 2020).

TABLE 5.1. Patient demographics

Number of Patients	105
Cochlear implant type (n)	
HiRes90K 1J	14
HiRes90K Mid-Scala	91
Age (years)	
Children (<16 years)	42
Mean age \pm SD (years)	5.2 \pm 3.6
Adults (\geq 16 years)	63
Mean age \pm SD (years)	61.8 \pm 15.9
Etiology (n)	
Medication	1
Meningitis	7
Otosclerosis	2
Congenital/Hereditary	35
Other/Unknown	60

SD represents standard deviation.

5.3 RESULTS

5.3.1 Extraction of S-eCAP and L-eCAP from R-eCAP

Each of the 2188 R-eCAP waveforms from 215 R-RRFs was split into an S-eCAP and an L-eCAP using iterative deconvolution. To test the validity of the deconvolution routine, the R-eCAPs were reconstructed from the S-eCAP and the L-eCAP by summation. The sum of the S- and L-eCAPs accurately reconstructed the R-eCAP, with median goodness of fit (i.e., the normalized root-mean-square error) of 91.7% (95% confidence interval: 89.5%–95.7%). A typical example of the extraction of the S-eCAP and L-eCAP is shown in Fig. 5.2. In this example, the summation of the S-eCAP and the L-eCAP matched the R-eCAP with a goodness of fit of

92.4%. One can directly see from this example that the latencies from the S-eCAP and L-eCAP are different, but also that the amplitude is far from that of the R-eCAP waveform. This illustrates that part of the response is canceled out of the summation of the responses due to the latency differences.

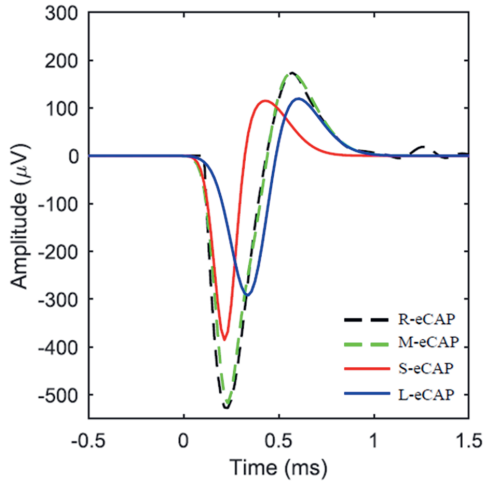


Fig. 5.2. A typical example of extracting the short-latency component (S-eCAP, the red solid line) and long-latency component (L-eCAP, the blue solid line) from the raw eCAP (R-eCAP, the black dashed line) of the raw eCAP refractory recovery function (R-RRF). The modeled eCAP (M-eCAP, the green dashed line) indicates the summation of the S-eCAP and the L-eCAP. eCAP: electrically evoked compound action potential.

5.3.2 The refractory parameters derived from the R-RRF, S-RRF, and L-RRF

Table 5.2 shows a descriptive analysis of the refractory parameters extracted from the R-RRF, S-RRF, and L-RRF, including measurements of central tendency (mean and median), and dispersion (median deviation). An example of the exponential fitting of the R-RRF, S-RRF, and L-RRF is shown in Fig. 5.3.

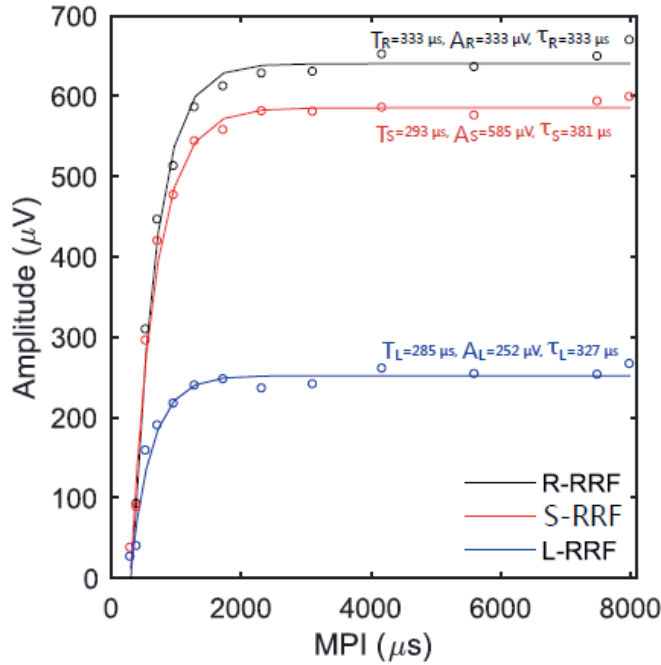


Fig. 5.3. Fitting the exponential model to the R-RRF, S-RRF, and L-RRF. R-RRF represents the recorded eCAP refractory recovery function; S-RRF and L-RRF represent the refractory recovery function of the short-latency and long-latency components in eCAPs. T is the absolute refractory period (in μs); A is the maximum eCAP amplitude at the maximum saturation level (in μV), and τ is the recovery time constant during the relative refractory period (in μs). T_R , A_R , and τ_R are for the R-RRF; T_S , A_S , and τ_S are for the S-RRF; T_L , A_L , and τ_L are for the L-RRF. MPI: the masker-probe interval. R-eCAP, S-eCAP, and L-eCAP are the same as for Fig. 5.1.

To test whether the refractory parameters derived from R-RRF, S-RRF, and L-RRF differed from each other, three LMMs were constructed for which T , A , and τ were entered as the dependent variable, respectively. In addition, a fixed variable was included that indicated whether R-RRF, S-RRF, or L-RRF was tested. All three LMMs showed a significant main effect of this fixed, categorical variable (T : $F(2, 547)=81.2$, $p<0.0001$; A : $F(2, 536)=299$, $p<0.0001$; and τ : $F(2,537)=4.1$, $p=0.004$, respectively). The contact number showed a significant effect on parameter T ($p=0.04$), A ($p<0.0001$) and τ ($p=0.02$).

Table 5.2. Descriptive statistics of the refractory parameters of the R-RRF, S-RRF, and L-RRF.

R-RRF, S-RRF, and L-RRF are the same as for Fig. 5.3. T_R , A_R , and τ_R are for the R-RRF; T_S , A_S , and τ_S are for the S-RRF; T_L , A_L , and τ_L are for the L-RRF. MD represents the median absolute deviation.

Refractory variables	Mean	Median	MD
T_R (μs)	368	366	85
T_S (μs)	306	300	29
T_L (μs)	285	229	38
A_R (μV)	432	390	159
A_S (μV)	426	385	164
A_L (μV)	220	184	105
τ_R (μs)	427	272	85
τ_S (μs)	529	338	211
τ_L (μs)	430	274	251

To compare how the refractory parameters T , A , and τ differed between the R-RRF, S-RRF, and L-RRF (see Eq. (5.2)), we used a post hoc t-test where the significance level was Bonferroni corrected to 0.017 (0.05 divided by 3 comparisons). For the absolute refractory period, T_R was significantly longer than T_S ($p < 0.001$) and T_L ($p < 0.001$), and T_S was significantly longer than T_L ($p < 0.001$). Regarding saturation level, A_R was significantly larger than A_S ($p = 0.011$) and A_L ($p < 0.0001$), and A_S was significantly larger than A_L ($p < 0.0001$). For the speed of recovery, we found that τ_S was significantly longer than τ_R ($p < 0.01$) and τ_L ($p < 0.01$), and no significant difference was observed between τ_R and τ_L ($p = 0.87$).

5.3.3 Comparisons of refractory parameters between children and adults

Table 5.3 shows the results of the descriptive analyses of the parameters between the two groups. We tested whether children and adults had different refractory characteristics by constructing nine LMMs with T_R , A_R , τ_R , T_S , A_S , τ_S , T_L , A_L , and τ_L entered as a dependent variable. For the absolute refractory period, T_R and T_S in children are significantly shorter than those in adults (T_R : $F(1, 92.3) = 10.4$, $p = 0.002$;), except for T_S ($F(1, 94.7) = 0.3$, $p = 0.9$) and T_L ($F(1, 95) = 0.19$, $p = 0.66$). Also, the saturation levels in children were significantly larger than those

of adults (A_R : $F(1, 96.5) = 5.0, p = 0.03$; A_S : $F(1, 97.8) = 4.4, p = 0.04$) except for A_L ($F(1, 102) = 4.1, p = 0.046$). Regarding the relative refractory period, no significant difference was observed between the two groups (τ_R : $F(1, 102.8) = 3.9, p = 0.05$; τ_S : $F(1, 101) = 0.8, p = 0.38$; and τ_L : $F(1, 105) = 0.9, p = 0.35$). The contact number showed a significant effect on parameters A_R, A_S, A_L ($p < 0.0001$) and τ_R ($p = 0.02$) but not on parameters $T_R, T_S, \tau_S, T_L,$ and τ_L (all $p > 0.05$).

Table 5.3. Descriptive results of the refractory parameters of children and adults. The parameters are the same as for Table 5.2. MD represents the median absolute deviation.

Variables	Children			Adults		
	Median	Mean	MD	Median	Mean	MD
T_R (μs)	349	334	101	392	392	92.5
T_S (μs)	352	353	93.3	397	401	70.5
T_L (μs)	370	360	110	405	428	85.8
A_R (μV)	446	470	67	353	393	178
A_S (μV)	438	452	118	339	375	181
A_L (μV)	224	218	71.9	157	181	63.7
τ_R (μs)	286	438	210	294	350	199
τ_S (μs)	208	347	273	237	229	182
τ_L (μs)	209	389	245	276	332	224

5.3.4 Relations between refractory parameters and speech perception

Nine LMMs were constructed to evaluate the association between speech perception and the refractory parameters ($T_R, T_S, T_L, A_R, A_S, A_L, \tau_R, \tau_S,$ and τ_L) in adult CI recipients by entering them as the dependent variable and the speech score as a fixed covariate in each model, respectively. The average word recognition score at the one-year follow-up in the 40 adult patients with CI was 58% words correct (range from 17% to 92%) and 72% phonemes correct (range from 46% to 98%). We found that only τ_S was significantly and negatively associated with word recognition score ($F(1, 53.2) = 6.5, p = 0.017$) and phoneme score ($F(1, 51.2) = 3.1,$

$p = 0.04$), taking contact location along the electrode array into consideration (Fig. 5.4). That is, patients with a higher speed of recovery of the S-eCAP tend to have better speech perception. However, regarding the remaining parameters, no significant associations were observed (all $p > 0.2$). In these LMMs, the contact number showed a significant effect on parameters A_R , A_S , and A_L ($p < 0.001$) but not on the other parameters (all $p > 0.1$).

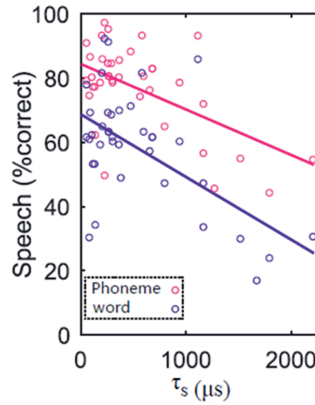


Fig. 5.4. Correlations between speech performance and the speed of recovery, τ_s . Scatterplots of recovery time constants (x -axis) plotted against the speech performance (y -axis).

5.4 DISCUSSION

Earlier studies suggested that human eCAPs include a short-latency component and a long-latency component, which are thought to arise from two different populations of ANFs. In the present study, we corroborated these findings by demonstrating the presence of two separate components in the human eCAP that have refractory characteristics that differ significantly from each other and from the raw eCAP. The refractory properties derived from S-RRF and L-RRF turned out to be of clinical relevance, because they differed significantly between children and adults and were significantly correlated with speech perception after cochlear implantation.

5.4.1 The refractory properties derived from the R-RRF, S-RRF, and L-RRF

We observed that the mean value of T_R was $368 \mu\text{s}$ and the mean value of τ_R was $427 \mu\text{s}$

(Table 5.2). Previous studies reported mean or median values of T_R and τ_R ranging from 276 to 650 μs and from 410 to 1480 μs , respectively (Dynes, 1996; Bruce et al., 1999; Boulet et al., 2015; Viemes et al., 2016; Carvalho et al., 2020); thus, we conclude that our results fall within the ranges reported in the existing literature. The refractory parameters of the S-eCAP and L-eCAP were significantly different from each other, and importantly, they were significantly different from those obtained from the R-RRF, except for τ_R and τ_L . These findings support the notion that the short-latency and long-latency components of the eCAP can be attributed to two different populations of ANFs with different refractory characteristics. According to the above, compared with S-eCAP and L-eCAP, the use of the directly measured R-eCAP is not likely to give a meaningful representation of the refractory properties of the AN which may obscure potential clinical implications.

5.4.2 Refractory characteristics of the AN in children and adults

The current study demonstrated a significantly shorter T_R and a significantly larger A_R in children than in adults, but there were no differences in τ_R between these groups. Our results were partially comparable with Carvalho et al. (2015), who found a significantly larger A_R in children than in adults. They did not find significant differences in T_R and τ_R between the two groups. Our results demonstrated that R-eCAP contains two different components with different refractory characteristics, and using S-eCAP and L-eCAP can lead to more accurate estimates of the refractory parameters. Thus, we further compared the refractory properties derived from the S-eCAP and L-eCAP between children and adults. Specifically, we only observed significant differences between the two groups for the S-RRF; namely, A_S was significantly larger in children. No significant differences between the two groups were observed for other parameters (T_S , T_L , A_L , τ_S , and τ_L). The result for A_S in our study was in line with the findings by Dong et al. (2020), who reported that a larger short-latency component of the compound discharge latency distribution, which is highly correlated to the eCAP amplitude, was observed in children. Gordon et al. (2002) also found higher eCAP amplitudes, i.e., ‘A’ values, in children compared with post-lingual adults. A possible explanation for the difference is that children have a larger

number of healthy ANFs involved in S-eCAP than adults.

In terms of speed of recovery, children did not demonstrate significant differences compared to adults (τ_S and τ_L) in our study. Our results did not support the finding by others that children tend to show a higher speed of recovery than adults (e.g., Xi et al., 2004). We believe that the inconsistent results observed in our study may have resulted from several factors, such as the different maturation of the ANFs and different duration of deafness between children and adults. Specifically, the AN in children is less mature than that in adults, such that children with CIs would undergo electrical impulses on the immature AN, and this might affect the maturation of the AN by the stimulation (e.g., Xu et al., 1997). In addition, hearing loss is usually age-related in adults, they tend to have suffered from deafness longer than children. As a consequence, adults have a greater risk of more extended nerve degeneration than children (e.g., Xi et al., 2004), and adults would expectedly have a lower speed of recovery. However, Botros and Psarros (2010) proposed that a larger neural ANF population, rather than a longer duration of deafness, would result in a lower speed of recovery. Thus, the existing literature is not in agreement on the presence of differences in the speed of recovery. The lack of any difference in our study may be caused by the mixture of the opposing influences of the maturation state, ANF population, and duration of deafness on the speed of recovery.

Shepherd et al. (2004) found that the absolute refractory period of individual rat auditory neurons increased with increasing duration of deafness. Our result of the T_S and T_L appear not to be in line with this expectation, i.e., adults do not show a longer absolute refractory period than children although adults usually suffered from longer periods of deafness. However, as stated above, we cannot rule out that the difference may be caused by the different populations and maturation of ANFs underlying S-eCAP and L-eCAP between the two groups. To further address if the refractory properties of ANFs of children differ from adults, maturation state, ANF population, and duration of deafness need to be taken into account in future studies.

5.4.3 Effects of auditory refractory properties on speech perception

In the present study, we observed that the τ_R did not show a significant relationship with speech perception. Previous literature reports equivocal results in terms of the importance of τ_R for speech recognition outcomes with a CI (e.g., He et al., 2017). We argue that the derived measures of the speed of recovery, S-RRF and L-RRF, are better estimates than the R-RRF measures, as we found a significant association between τ_S and speech perception. One possible explanation was that two components in the eCAP originated from different populations of ANFs in terms of degenerative state, maturation, and refractory characteristics. For instance, the S-eCAP may arise from a healthier group of fibers and the L-eCAP from a more degenerated group, representing different surviving and functional statuses (e.g., Ramekers et al., 2015; Konerding et al., 2020). Therefore, the two populations of ANFs can affect speech perception differently, namely, the speed of recovery derived from the S-eCAP contributes significantly more to speech performance than that from L-eCAP. Importantly, the speed of recovery obtained by the conventional R-RRF using the raw eCAP amplitude does not predict performance, while considering the S- and L-eCAP separately proved to yield a more useful indicator for the CI outcomes. Furthermore, the results that the T and A parameters of R-RRF, S-RRF, and L-RRF did not correlate to speech perception suggested that they appear not to be essential factors for speech performance. Therefore, we advise the use of the derived S-RRF and L-RRF components instead of R-RRF in future clinical practice to predict speech performance after implantation.

A limitation of this study is that realistic refractory parameters of 29 RRFs (13.9%) could not be derived due to fitting errors. Morsnowski et al. (2005) also reported that 9 of 71 (12%) stimulation sites resulted in fitting errors. We believe that the possible reasons behind the failure may be the recording technique, as parameter estimates are likely to be sensitive to the number of data points; the MPI axis values; and the ANF density (Shepherd et al., 2004; Cohen, 2009; Boulet et al., 2015; He et al., 2017). The stability and validity of the exponential decay fitting of RRF (Eq. (5.1)) are sensitive to the number of data points and the MPI axis values, especially within the relative refractory period. For instance, when eCAPs cannot be detected due to

background noise in the recording, the missing data likely result in a parameter discrepancy. It is possible that future studies, especially with additional MPIs within the relative refractory period, may refine the present estimates of the refractory characteristics of the whole nerve. In addition, uncertainty remains regarding the origins of the S-eCAP and L-eCAP (e.g., Strahl et al., 2016; Dong et al., 2020) and the physiological mechanism of the different refractory properties underlying the S-eCAP and L-eCAP. To further understand these issues, future studies with electrophysiological measures of the AN are warranted.

5.5 CONCLUSIONS

In the current study, we demonstrated that the short-latency and long-latency components of the eCAP have different auditory refractory properties. The refractory properties of the two eCAP components differed between children and adults. Importantly, the speed of recovery, as obtained by the classical RRF method using the raw eCAP, did not predict speech performance. However, evaluating the two components of the eCAP separately proved to be indicative of speech performance after implantation. The collective results suggest that consideration should be given to the two components of the eCAP separately when the AN refractory characteristics are evaluated for clinical purposes.

ACKNOWLEDGMENTS

The first author of the present study is financially supported by the China Scholarship Council. There are no conflicts of interest, financial or otherwise.

Yu Dong designed and performed experiments, analyzed data, and wrote the paper; Jeroen J. Briaire designed experiments, discussed the results and implications, and provided critical revision; H. Christiaan Stronks and Johan H. M. Frijns discussed the results and implications and provided critical revision.

REFERENCES

- Abbas, P. J., & Brown, C. J. (1991). Electrically evoked auditory brainstem response: refractory properties and strength-duration functions. *Hearing research*, 51(1), 139-147.
- Battmer, R. D., Lai, W. K., Dillier, N., Pesch, J., Killian, M. J., & Lenarz, T. (2005). Correlation of NRT recovery function parameters and speech perception results for different stimulation rates. In *Abstracts of the Fourth International Symposium and Workshops on Objective Measures in Cochlear Implants* (p. 21).
- Biesheuvel, J. D., Briaire, J. J., & Frijns, J. H. (2018). The precision of eCAP thresholds derived from amplitude growth functions. *Ear and hearing*, 39(4), 701-711.
- Bosman, A. J., & Smoorenburg, G. F. (1995). Intelligibility of Dutch CVC syllables and sentences for listeners with normal hearing and with three types of hearing impairment. *Audiology*, 34(5), 260-284.
- Botros, A., & Psarros, C. (2010). Neural Response Telemetry Reconsidered: II. The Influence of Neural Population on the ECAP Recovery Function and Refractoriness. *Ear & Hearing*, 31(3), 380-391.
- Boulet, J., White, M., & Bruce, I. C. (2016). Temporal Considerations for Stimulating Spiral Ganglion Neurons with Cochlear Implants. *JARO - Journal of the Association for Research in Otolaryngology*, 17(1), 1-17.
- Brauer, M., Curtin, J. J. (2018). Linear mixed-effects models and the analysis of nonindependent data: A unified framework to analyze categorical and continuous independent variables that vary within-subjects and/or within-items. *Psychol Methods*, 23, 389-411.
- Brown, C. J., Abbas, P. J., & Gantz, B. (1990). Electrically evoked whole-nerve action potentials: Data from human cochlear implant users. *The Journal of the Acoustical Society of America*, 88(3), 1385-1391.
- Bruce, I. C., Irlicht, L. S., White, M. W., O'Leary, S. J., Dynes, S., Javel, E., & Clark, G. M. (1999). A stochastic model of the electrically stimulated AN: pulse-train response. *IEEE Transactions on Biomedical Engineering*, 46(6), 630-637.
- Cohen, S. M., & Svirsky, M. A. (2019). Duration of unilateral auditory deprivation is associated with reduced speech perception after cochlear implantation: A single-sided deafness study. *Cochlear Implants International*, 20(2), 51-56.
- Dong, Y., Briaire, J. J., Biesheuvel, J. D., Stronks, H. C., & Frijns, J. H. M. (2020). Unravelling the Temporal Properties of Human eCAPs through an Iterative Deconvolution Model. *Hearing Research*, 395, 108037.

- Dong, Y., Stronks, H. C., Briaire, J. J., & Frijns, J. H. (2021). An iterative deconvolution model to extract the temporal firing properties of the auditory nerve fibers in human eCAPs. *MethodsX*, 8, 101240.
- Dynes, S. B. C. (1996). Discharge characteristics of auditory nerve fibers for pulsatile electrical stimuli (Doctoral dissertation, Massachusetts Institute of Technology).
- Fitzmaurice, G. M., Laird, N. M., & Ware, J. J. (2004). Linear mixed effects models. *Applied longitudinal analysis*, 1, 187-236.
- Fulmer, S. L., Runge, C. L., Jensen, J. W., & Friedland, D. R. (2011). Rate of neural recovery in implanted children with auditory neuropathy spectrum disorder. *Otolaryngology-Head and Neck Surgery*, 144(2), 274–279.
- Gantz, B. J., Brown, C. J., & Abbas, P. J. (1994). Intraoperative measures of electrically evoked AN compound action potential. *The American journal of otology*, 15(2), 137-144.
- Gray, P. R. (1967). Conditional probability analyses of the spike activity of single neurons. *Biophysical Journal*, 7(6), 759-777.
- Gordon, K. A., Gilden, J. E., Ebinger, K. A., & Shapiro, W. H. (2002). Neural response telemetry in 12- to 24-month-old children. *Annals of Otolaryngology, Rhinology & Laryngology*, 111(5_suppl), 42-48.
- He, S., Teagle, H. F. B., & Buchman, C. A. (2017). The electrically evoked compound action potential: From laboratory to clinic. *Frontiers in Neuroscience*, 11(JUN), 1–20.
- Kiefer, J., Hohl, S., Stürzebecher, E., Pfennigdorff, T., & Gstöettner, W. (2001). Comparison of speech recognition with different speech coding strategies (SPEAK, CIS, and ACE) and their relationship to telemetric measures of compound action potentials in the nucleus CI 24M cochlear implant system. *International Journal of Audiology*, 40(1), 32–42.
- Lai, W. K., & Dillier, N. (2000). A Simple Two-Component Model of the Electrically Evoked Compound Action Potential in the Human Cochlea. *Audiology and Neurotology*, 5(6), 333–345.
- Lee, E. R., Friedland, D. R., & Runge, C. L. (2012). Recovery from forward masking in elderly cochlear implant users. *Otology and Neurotology*, 33(3), 355–363.
- Matsuoka, A. J., Rubinstein, J. T., Abbas, P. J., & Miller, C. A. (2001). The effects of interpulse interval on stochastic properties of electrical stimulation: models and measurements. *IEEE transactions on biomedical engineering*, 48(4), 416-424.
- Miller, C. A., Abbas, P. J., & Brown, C. J. (2000). An improved method of reducing stimulus artifact in the electrically evoked whole-nerve potential. In *Ear and Hearing* (Vol. 21, Issue 4, pp. 280–290).
- Miller, C. A., Abbas, P. J., & Robinson, B. K. (2001). Response properties of the refractory AN fiber. *JARO - Journal of the Association for Research in Otolaryngology*, 2(3), 216–232.

- Molenberghs, G., Bijmens, L., Shaw, D. (1997) Linear Mixed Models and Missing Data. In: *Linear Mixed Models in Practice. Lecture Notes in Statistics*, vol 126. Springer, New York, NY. https://doi.org/10.1007/978-1-4612-2294-1_5
- Morsnowski, A., Charasse, B., Collet, L., Killian, M., & Müller-Deile, J. (2006). Measuring the refractoriness of the electrically stimulated AN. *Audiology and Neurotology*, 11(6), 389–402.
- Ramekers, D., Versnel, H., Strahl, S. B., Klis, S. F. L., & Grolman, W. (2015). Recovery characteristics of the electrically stimulated AN in deafened guinea pigs: Relation to neuronal status. *Hearing Research*, 321, 12–24.
- Shepherd, R.K. & Hardie, N.A. (2001). Deafness-induced changes in the auditory pathway: implications for cochlear implants. *Audiol. Neurootol.*, 6, 305–318.
- Shepherd, R. K., Roberts, L. A., & Paolini, A. G. (2004). Long-term sensorineural hearing loss induces functional changes in the rat auditory nerve. *European Journal of Neuroscience*, 20(11), 3131-3140.
- Strahl, S. B., Ramekers, D., Nagelkerke, M. M., Schwarz, K. E., Spitzer, P., Klis, S. F., ... & Versnel, H. (2016). Assessing the firing properties of the electrically stimulated auditory nerve using a convolution model. In *Physiology, Psychoacoustics and Cognition in Normal and Impaired Hearing* (pp. 143-153). Springer, Cham.
- Stypulkowski, P. H., & van den Honert, C. (1984a). Physiological properties of the electrically stimulated AN. I. Compound action potential recordings. *Hearing Research*, 14(3), 205–223.
- van den Honert, C., & Stypulkowski, P. H. (1984b). Physiological properties of the electrically stimulated auditory nerve. II. Single fiber recordings. *Hearing Research*, 14(3), 225–243.
- Versnel, H., Prijs, V. F., & Schoonhoven, R. (1992). Round-window recorded potential of single-fibre discharge (unit response) in normal and noise-damaged cochleas. *Hearing Research*, 59(2), 157–170. [https://doi.org/10.1016/0378-5955\(92\)90112-Z](https://doi.org/10.1016/0378-5955(92)90112-Z)
- Turner, C., Mehr, M., Hughes, M., Brown, C., & Abbas, P. (2002). Within-subject predictors of speech recognition in cochlear implants: A null result. *Acoustic Research Letters Online*, 3, 95–100.
- van de Heyning, P., Arauz, S. L., Atlas, M., Baumgartner, W. D., Caversaccio, M., Chester-Browne, R., et al. (2016). Electrically evoked compound action potentials are different depending on the site of cochlear stimulation. *Cochlear Implants Int.* 17, 251–262.
- Van Eijl, R. H. M., Buitenhuis, P. J., Stegeman, I., Klis, S. F. L., & Grolman, W. (2017). Systematic review of compound action potentials as predictors for cochlear implant performance. *Laryngoscope*, 127(2), 476–487.
- Wilson, B. S., Finley, C. C., Lawson, D. T., and Zerbi, M. (1994). *Speech Processors for Auditory Prostheses*. NIH Project N01-DC-2-2401. Seventh Quarterly Progress Report.

- Xi, X., Ji, F., Han, D. Y., Huang, D. L., Hong, M. D., & Yang, W. Y. (2004). Refractory recovery function of electrical auditory on the survival auditory nerve in cochlear implant recipients. *Zhonghua er bi yan hou ke za zhi*, 39(2), 77-80.
- Xu, J., Shepherd, R. K., Millard, R. E., & Clark, G. M. (1997). Chronic electrical stimulation of the auditory nerve at high stimulus rates: a physiological and histopathological study. *Hearing research*, 105(1-2), 1-29